J. Membrane Biol. 165, 243–254 (1998)

The Journal of
Membrane
Biology

Freeze-Fracture Analysis of Plasma Membranes of CHO Cells Stably Expressing Aquaporins 1-5

A.N. van Hoek[1], **B. Yang**[2], **S. Kirmiz**[2], **D. Brown**[1]

[1]Renal Unit and Department of Pathology, Massachusetts General Hospital and Harvard Medical School, Boston, MA 02114, USA
[2]Departments of Medicine and Physiology, Cardiovascular Research Institute, University of California, San Francisco, CA 94143, USA

Received: 17 March 1998/Revised: 19 June 1998

Abstract. Several studies suggest that aquaporin water channels can be identified in membranes by freeze-fracture electron microscopy. For this report, Chinese Hamster ovary cells were stably transfected with cDNAs encoding aquaporins 1–5. Measurement of the osmotic water permeability of the cells confirmed that functional protein was expressed and delivered to the plasma membrane. By freeze-fracture electron microscopy, a 20% increase in intramembrane particle (IMP) density was found in plasma membranes of cells expressing AQP2, 3 and 5, and a 100% increase was measured in AQP1-expressing cells, when compared to mock-transfected cells. On membranes of cells expressing AQP4, large aggregates of IMPs were organized into orthogonal arrays, which occupied 10–20% of the membrane surface. IMP aggregates were never seen in AQP2-transfected cells. Hexagonally packed IMP clusters were detected in ~5% of the membranes from AQP3-expressing cells. Particle size-distribution analysis of rotary shadowed IMPs showed a significant shift from 13.5 (control cells) to 8.5 nm or less in AQP-expressing cells; size distribution analysis of unidirectionally shadowed IMPs also showed a significant change when compared to control. Some IMPs in AQP expressing cells had features consistent with the idea that aquaporins are assembled as tetramers. The results demonstrate that in transfected CHO cells, AQP transfection modifies the general appearance and number of IMPs on the plasma membrane, and show that only AQP4 assembles into well-defined IMP arrays.

Key words: Freeze fracture — Orthogonal, square array — Intramembrane particle — Aquaporin — Chinese Hamster ovary cell — Transfection

Correspondence to: A.N. van Hoek

Introduction

Facilitated water transporting pathways associated with the presence of aquaporins have been reported in epithelial cells from various regions of the nephron, as well as in many other tissues and cell types, including erythrocytes, trachea, lung, sweat glands, epidermis, spinal cord, brain, stomach, reproductive organs, mammalian and amphibian urinary bladder, and amphibian epidermis (Van Os, Deen & Dempster, 1994; Agre, Brown & Nielsen, 1995; Knepper et al., 1996; Verkman et al., 1996). Long before the aquaporin family of water channels was identified, characteristic aggregates of intramembrane particles (IMPs), observed by freeze-fracture EM, were identified in the membranes of vasopressin-sensitive cell types in amphibian urinary bladder and epidermis, and in collecting duct principal cells after hormonal stimulation (Chevalier, Bourguet & Hugon, 1974; Humbert et al., 1975; Kachadorian, Wade & DiScala, 1975; Harmanci et al., 1978, 1980; Brown & Orci, 1983). It was first proposed by Chevalier et al. (1974) that these IMP aggregates in the frog urinary bladder might represent water transporting units and a significant amount of correlative structural/functional data subsequently supported this contention. While the phenomenon of IMP aggregates appearing in plasma membranes in parallel with an increase in water permeability is common to these three hormonally responsive cell types, the morphological organization of the aggregates, as visualized by freeze-fracture, is different in all three cell types (Brown, 1991). In amphibian bladder, the aggregates are tightly packed on the membrane P-face, but form linear, parallel arrays of grooves on the complementary E-face. In collecting duct principal cells, the aggregates (Harmanci et al., 1978, 1980) are less tightly packed, appearing as loose IMP clusters on both P- and E-faces. Finally, the aggregates in toad epidermis form

geometrically packed orthogonal arrays (Brown, Grosso & DeSousa, 1983). Similar orthogonal (or square) arrays are present in numerous plasma membranes of other cell types, including intestinal epithelial cells (Staehelin, 1972), gastric parietal cells (Bordi & Perrelet, 1978), sarcolemmas of fast twitch muscle fibers (Ellisman et al., 1976, Schmalbruch, 1979), type I alveolar cells (Bartels, 1979), astrocytic plasma membranes apposed to blood vessels and to the cerebrospinal fluid at the surface of the brain (Landis & Reese, 1981), the basolateral plasma membrane of collecting duct principal cells (Orci et al., 1981), the lateral membrane of inner hair cells (Forge, 1987), tracheal epithelium (Widdicombe et al., 1987), ciliary epithelium (Hirsch, Gache & Noske, 1988), the vestibular sensory epithelium (Saito, 1988) and, most strikingly, in lens fibers (Zampighi et al., 1982).

The archetypal member of a growing group of homologous mammalian aquaporins, lens protein MIP26 (AQP0), which has a low water permeability, has been shown to form orthogonal arrays of particles in lens-fiber membranes (Ehring et al., 1990). The water channel aquaporin-1 (AQP1) from erythrocytes and proximal tubule forms tetramers in native membranes and AQP1-expressing CHO cells, and does not appear to assemble into higher-order aggregates (Verbavatz et al., 1993). In contrast, morphological and tissue distribution studies of the AQP4 protein suggested that AQP4 forms orthogonal IMP arrays in the basolateral plasma membrane of kidney collecting duct, astrocytes in brain and spinal cord, and epithelial cells in stomach, trachea, bronchi, intestine, ciliary body and various exocrine glands (Frigeri et al., 1995). The ability of AQP4 to form orthogonal IMP arrays was confirmed by the finding that orthogonal IMP arrays were present on plasma membranes of AQP4-expressing CHO cells (Yang, Brown & Verkman, 1995). Other evidence that AQP4 is an orthogonal array forming protein came from studies on AQP4-knock-out mice showing the absence of OAPs in brain, muscle and kidney (Verbavatz et al., 1997).

Little is known about the tertiary structure of other water channels. In particular, it is not known whether AQP2, the vasopressin-sensitive water channel, can form IMP aggregates or clusters when expressed in mammalian cells. Also, while two members of the MIP family have been shown to form orthogonal IMP arrays, not all known OAPs have been identified. In addition, functional studies of epitope-tagged aquaporins 1–5 revealed different single channel water permeabilities when expressed in oocytes (Yang & Verkman, 1997), and some aquaporins function not only as water channels, but also as solute transporters (e.g., AQP3, AQP8, AQP9). Each aquaporin could thus have a different oligomeric structure. The purpose of this study was to investigate the morphology of aquaporins 1 through 5 in stably transfected CHO cells by unidirectional and rotary shadowing of freeze-fractured CHO cell plasma membranes. The major finding is that only AQP4 expression results in the appearance of abundant IMP aggregates that take the form of orthogonal arrays, as previously reported, while some aggregates of 10×10 nm^2 were observed in AQP3-expressing cells.

Materials and Methods

Cell Culture and Transfection

Chinese Hamster ovary (CHO) cells were transfected with rat AQPs 1–5 as described previously (Ma et al., 1993; Yang et al., 1996; Farinas et al., 1997). Mock-transfected CHO cells were generated by transfection with empty vector. Homogeneous populations of stably transfected cells were obtained by selection with G418 and cloning individual colonies. Cell clones with the highest water permeabilities were used for morphological measurements. Cells were grown to near confluence on 6-well plastic dishes, fixed for 4 hr in 2% glutaraldehyde, and stored in PBS containing sodium azide.

Water Permeability Measurements

Osmotic water permeability was measured in near-confluent CHO cell layers cultured on 18 mm diameter round coverglasses. Coverglasses were mounted in a perfusion chamber for rapid exchange of bathing osmolality between 300 mOsm (PBS) and 150 mOsm (PBS diluted with water). The time course of cell volume change was measured by spatial filtering microscopy (Farinas et al., 1997), which utilizes cell volume-dependent changes in intracellular refractive index to infer cell volume. Relative water permeabilities were determined by single exponential regression of the time course data.

Fixation and Freeze-Fracture Analysis

Unidirectional and rotary shadowing of freeze-fractured membranes were carried out on transfected CHO-cells that were fixed for 4 hr in 2% glutaraldehyde, washed twice with PBS and cryoprotected with 30% glycerol in 0.1 Na-cacodylate (pH 7.5) buffer. The cells that were grown on plastic 6-well plates were scraped off after incubation overnight with the cryoprotectant. Aliquots of cell suspensions were placed on copper specimen holders and frozen by immersion in N_2-cooled Freon 22, at the transition temperature of liquified-solidified Freon 22. The frozen samples were rapidly transferred into a Cressington freeze-fracture apparatus (Cressington Scientific Instruments, Watford, U.K.). The temperature of the samples was increased to −120°C to remove Freon 22 and the membranes were fractured after approximately 20 min under a vacuum of 10^{-7} Torr. Specimens were shadowed with platinum at a 45° angle. A 1.5 nm film was deposited without specimen rotation (unidirectional shadowing), while a 2 nm coat was utilized for rotary shadowing. The platinum shadowing was followed by deposition of a 5 nm carbon coat perpendicular to the fracture plane. After the removal of the sample from the Cressington chamber, the specimen was removed from the copper support in sodium hypochlorite bleach. Replicas were further cleaned by several rinses in distilled water. The replicas were picked up on nickel grids and examined in a Philips CM10 electron microscope (Mahwah, NJ).

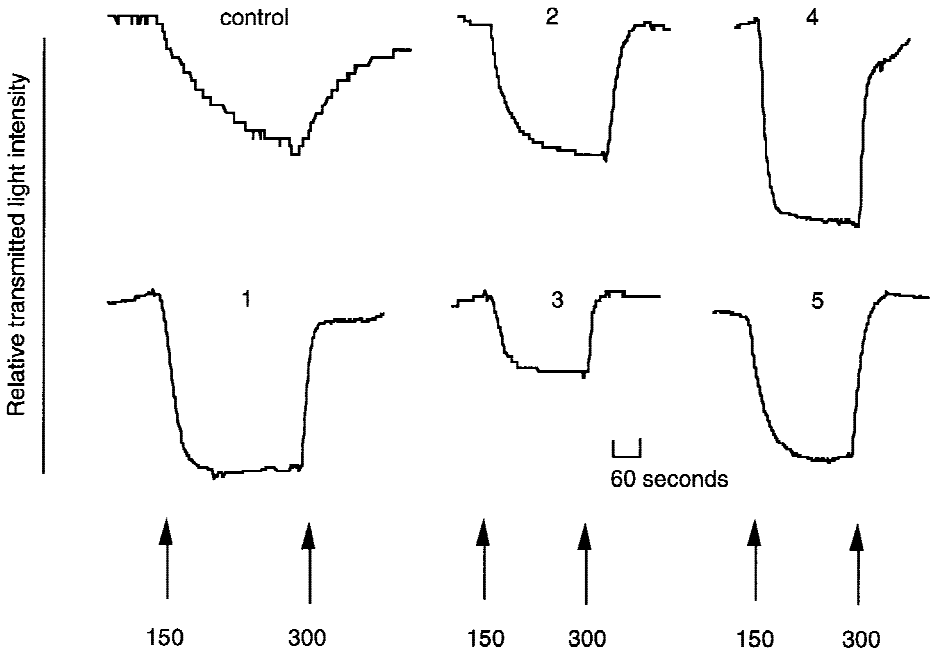

Fig. 1. Functional analysis of stably transfected CHO cells. The time course of relative cell volume was measured by spatial filtering microscopy as described previously (Farinas et al., 1997). Cells were originally bathed in PBS (300 mOsm) and then the perfusate was changed to PBS:water (2:1, 200 mOsm) and then back to PBS. Solution temperature was maintained at 23°C. The number above the trace corresponds to the aquaporin expressed in CHO-cells.

Quantification of IMP Density and Size

Fractured membranes were photographed after the specimen tilt in the microscope was minimized by adjusting the EM-specimen holder (eucentric height) to reduce overestimation of the particle density and minimize errors in the determination of particle size. The protoplasmic (P) and exoplasmic (E) face IMP densities were measured on plasma membrane areas of 0.5 × 0.5 μm^2 at 72,000 magnification of unidirectionally shadowed replicas. Some rotary shadowed samples were utilized for comparison, and the values obtained did not differ significantly from the samples that were shadowed unidirectionally. A total of 10 to 25 cell membranes from each CHO cell type were subjected to the procedure. Particle density measurements of AQP4-expressing cells may be compromised, because of the tight packing of particles into orthogonal arrays. The number of OAPs in a typical membrane was 5 per square micron, occupying about 10–20% of the total membrane area. With the center to center spacing of 6.8 nm, representing a membrane particle, ~200 of these particles will fit in an area of 100 × 100 nm (1% of a square micron). Thus AQP4 alone would account for ~2000 IMPs per square micron (10% area occupation), while randomly chosen area's of P-faces revealed a mean size of ~1800 particles per square micron (*see* Results). The last number was utilized, also to construct the size frequency diagrams for AQP4-expressing cells. IMP diameters were measured on photographs at 630,000× magnification. The width of the electron dense deposit was measured from unidirectionally shadowed particles at right angles to the direction of shadowing. The diameter of rotary shadowed particles was also measured. Half of the thickness of the brightly shadowed rim surrounding the IMP was included in this size measurement. The diameter distribution was fitted to one of two Gaussian functions of the form:

$$y = \sum_i \alpha_i e^{-(x-\beta_i)^2/\sigma_i^2},$$

where x is IMP diameter and y is density.

Abbreviations

CHO cell:	Chinese Hamster ovary cell
AQP:	aquaporin
IMP:	intramembrane particle
OAP:	orthogonal array particle
P–face:	protoplasmic face
E–face:	ectoplasmic face

Results

To confirm the expression of each aquaporin in the CHO cell plasma membrane, cell osmotic water permeability was measured by an optical method. CHO cells grown on coverglasses were subjected to osmotic gradients and the time course of cell volume change was determined (Fig. 1). The mock-transfected CHO cells swelled and shrunk slowly in response to osmotic gradients. In contrast, the rate of swelling and shrinking was >5-fold increased in CHO cells expressing each of the aquaporins. Because the time course of the cell volume change is limited by the perfusion rate of the bathing solution when AQPs are expressed, the absolute osmotic water permeability coefficient in each of the cell types could not be accurately determined under these experimental conditions. Temperature dependence measurements (at 12, 23 and 37°C) indicated a low Arrhenius activation energy

(*not shown*), consistent with water movement via the aquaporins. These results indicate that the AQP-transfected cells expressed functional aquaporins at their cell surface.

Unidirectional Shadowing

Figure 2 is a composite of micrographs representing the appearance of the plasma membrane P-face of control and aquaporin-expressing CHO cells after unidirectional shadowing. In all cells examined, the density of intramembrane particles (IMPs) was higher on protoplasmic fracture faces (P-faces) than on the complementary exoplasmic fracture faces (E-face, *not shown*), as is commonly seen for biological membranes. The P-face of control, mock-transfected cells exhibited a population of dispersed IMPs (Fig. 2*A*). Cells expressing AQP1 (*B*), AQP2 (*C*) and AQP5 (*F*) showed a pattern of IMP distribution in P-face that was also scattered throughout the plane of the membrane, although the number of IMPs was greater than in mock transfected CHO cells. In contrast, the P-face of cells expressing AQP4 displayed numerous large aggregates of IMPs (Fig. 2*E*). These IMP arrays were identical to the orthogonal arrays that have previously been correlated with AQP4 expression in a variety of cell types (Frigeri et al., 1995). Cells expressing AQP3 (Fig. 2*D*) showed mainly dispersed IMPs, but in some cells, packed clusters of IMPs with dimensions of 1.0 × 0.1 μm were also found. These small clusters were only found in ~5% of the cells examined, and they were only seen in cells transfected with AQP3, but never in control cells nor in cells expressing the other aquaporins.

Higher magnification (Fig. 3) revealed more details of AQP3-clusters and AQP4-OAPs. Figure 3*A* from an AQP3-expressing cell displays an aggregate of 30 to 40 subunits in shape forming an irregular cluster of IMPs on the P-face. On the E-face, complementary imprints probably corresponding to the P-face clusters were found (Fig. 3*B*). These imprints indicated a hexagonal packing of IMPs with a center-to-center spacing of ~8.5 nm. For AQP4 arrays, a center-to-center spacing of 6.8 nm was measured for the individual IMP units or impressions in both P-faces (Fig. 3*C*) and E-faces (Fig. 3*D*), respectively. The E-face imprints appeared as a series of linear arrays of grooves or checker boards depending on the direction of platinum shadowing with respect to the orientation of the array.

A quantitative evaluation of IMP number is shown in Table 1. Not every aquaporin transfection led to a large increase of IMP density in the plasma membrane, as was reported for AQP1 (Verbavatz et al., 1993). AQP1 transfection resulted in a doubling of IMP density, while AQP2, AQP3, and AQP5 gave only small increases in density (about 20%). The counting method to obtain IMP number could not be utilized for AQP4 with confidence, because large areas in both P- and E- faces were occupied by OAPs. Additional information on the expression of aquaporins was obtained by determining sizes and size distributions of IMPs in P-faces, utilizing images of unidirectionally shadowed membranes at higher magnification (Fig. 4).

Inspection of the micrographs indicated some additional differences. CHO cells expressing AQP1 (Fig. 4*B*) and AQP2 (Fig. 4*C*) gave IMP sizes that were significantly greater than those observed in mock transfected cells (Fig. 4*A*). AQP3 (Fig. 4*D*) expressing cells had also larger IMPs and a tendency of clustering of some of these IMPs. AQP5 (Fig. 4*F*) expressing cells had IMP populations that were apparently heterogeneous in size. Particles located outside OAPs of AQP4 expressing cells (Fig. 4*E*) appeared to have a similar size to the smaller particles found in AQP3 and AQP5 expressing cells. Figure 5 shows a size analysis, and Table 2 provides the fitted statistical parameters. The Gaussian distributions of AQP3 and AQP5 suggest two major populations of smaller and larger particles, different from the populations found in mock-transfected cells. A homogeneous distribution of larger particles was measured in AQP1 and AQP2 transfected cells. Although apparent diversity is seen among AQP-expressing cells, the difference between mock and AQP expression suggests that expression of endogenous membrane proteins is modified by AQP expression.

Rotary-Shadow Freeze-Fracture Analysis

Rotary shadowed freeze fracture analysis has been valuable for determining the ''subunit'' morphology of AQP1 in proteoliposomes, revealing an apparent tetrameric assembly of 4 smaller subunits. Similar structures were observed on the plasma membrane of AQP1 expressing CHO cells (Verbavatz et al., 1993). Figure 6 is a composite of micrographs representing the appearance of the plasma membrane P-face of control and aquaporin-expressing CHO cells after rotary shadowing. The contrast between IMPs and the lipid bilayer is somewhat diminished, but reveals more details of IMP structure and organization. IMPs protruding from the membrane leaflet appear as islands in the membrane surrounded by a brighter shadow boundary of less electron-dense deposits. The majority of IMPs in untransfected cells were different from the IMPs found in AQP-expressing cells. They almost blended with the membrane with a small recognizable brighter rim circumscribing in many cases apparently hexagonal structures. IMPs of AQP1 (Fig. 6*B*) expressing cells looked in general smaller and some had a tetrameric configuration previously ascribed to AQP1 (Verbavatz et al., 1993). Most IMPs of AQP2 expressing cells (Fig. 6*C*) appeared

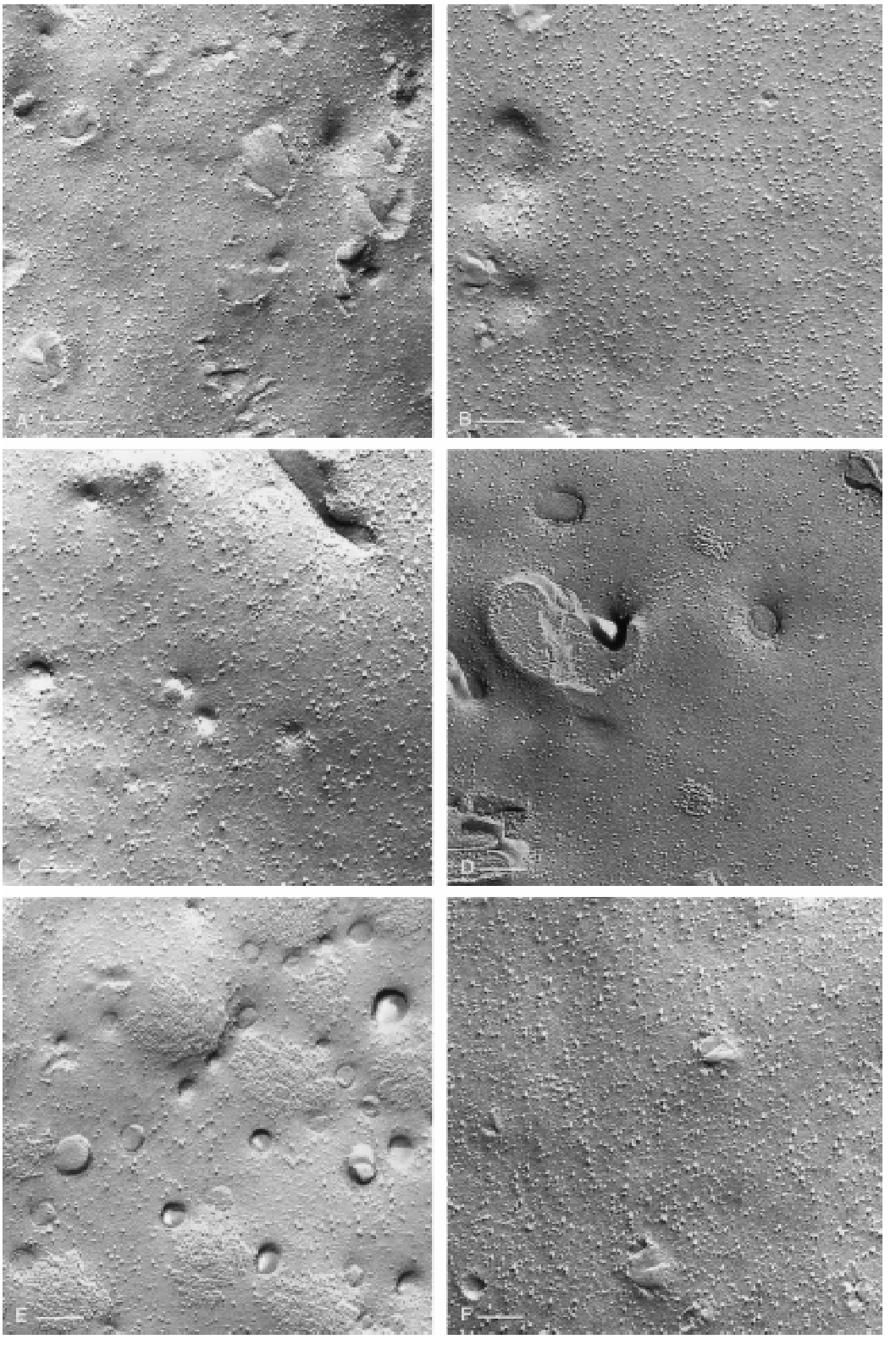

Fig. 2. Freeze-fracture electron micrographs of CHO cell plasma membranes expressing aquaporins. P-faces obtained after freeze-fracture were replicated by unidirectional shadowing with platinum. (*A*) mock-transfected cells; (*B*) AQP1-expressing cells; (*C*) AQP2-, (*D*) AQP3-, (*E*) AQP4-, and (*F*) AQP5-expressing cells. Note *D* which contains compact clusters of irregularly arranged IMPs, while in *E* large OAPs on the P-face are arranged in an square array. *Bars,* 100 nm.

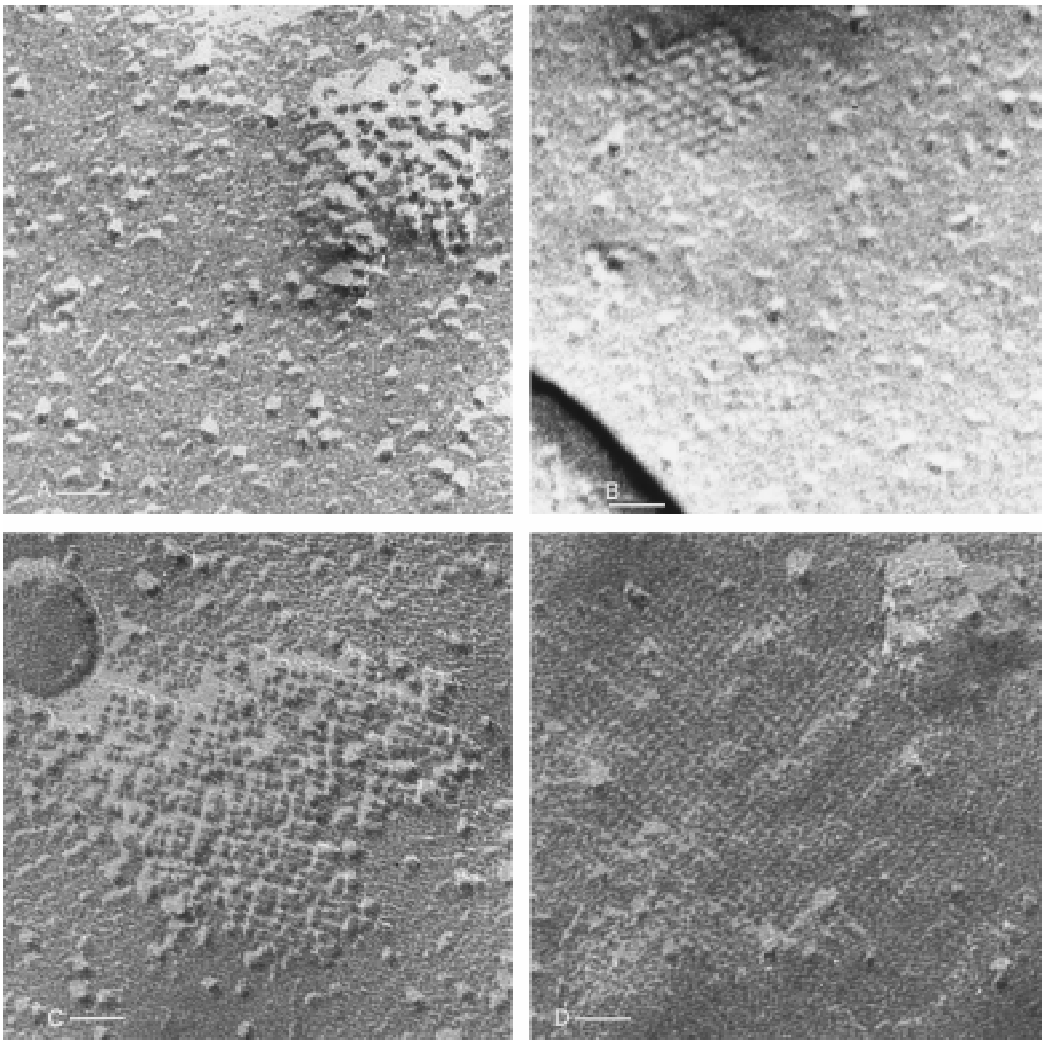

Fig. 3. High magnification of unidirectionally shadowed freeze-fractured electron micrographs of CHO cells expressing AQP3 and AQP4. (*A*) A cluster of P-face IMPs AQP3-expressing cells exhibits an assembly of ~40 units. (*B*) A lattice-like structure in E-face of AQP3-expressing cells with a hexagonal arrangement of imprints. (*C*) IMP aggregate (OAP) in P-face of AQP4-expressing cells. (*D*) A complementary imprint of OAPs in E-face of AQP4 expressing cells. *Bars*, 30 nm.

to be even smaller, some showing subunit features consistent with a tetrameric configuration. Some IMPs in AQP3 expressing cells (Fig. 6*D*) appeared as structures raised from the fracture plane. In some of the IMPs from OAP forming aggregates, an oligomeric configuration of 4 subunits could be distinguished (Fig. 6*E*). IMPs of AQP5 (Fig. 6*F*) expressing cells had a globular appearance.

IMP densities measured from rotary-shadowed replicas were not significantly diffferent from unidirectionally shadowed membranes. However, the IMP sizes measured after rotary shadowing showed unexpected differences from unidirectional shadowing. A clear difference between control and aquaporin-expressing cells was

Table 1. Particle density of aquaporins in plasma membranes of stably transfected CHO cells

Transfected CHO cells	Density of E-face IMPs			Density of P-face IMPs		
	(*IMP*s/μm^2)	(SD)	(*n*)	(*IMP*s/μm^2)	(SD)	(*n*)
Mock	408	±264	(10)	1258	±313	(24)
AQP1	340	±110	(12)	2428	±185	(15)
AQP2	511	±310	(11)	1504	±150	(21)
AQP3	345	±106	(13)	1580	±211	(19)
AQP4	186	±104	(12)	1791	±258	(23)
AQP5	475	±202	(14)	1575	±146	(17)

n is the number of membranes used to determine density.

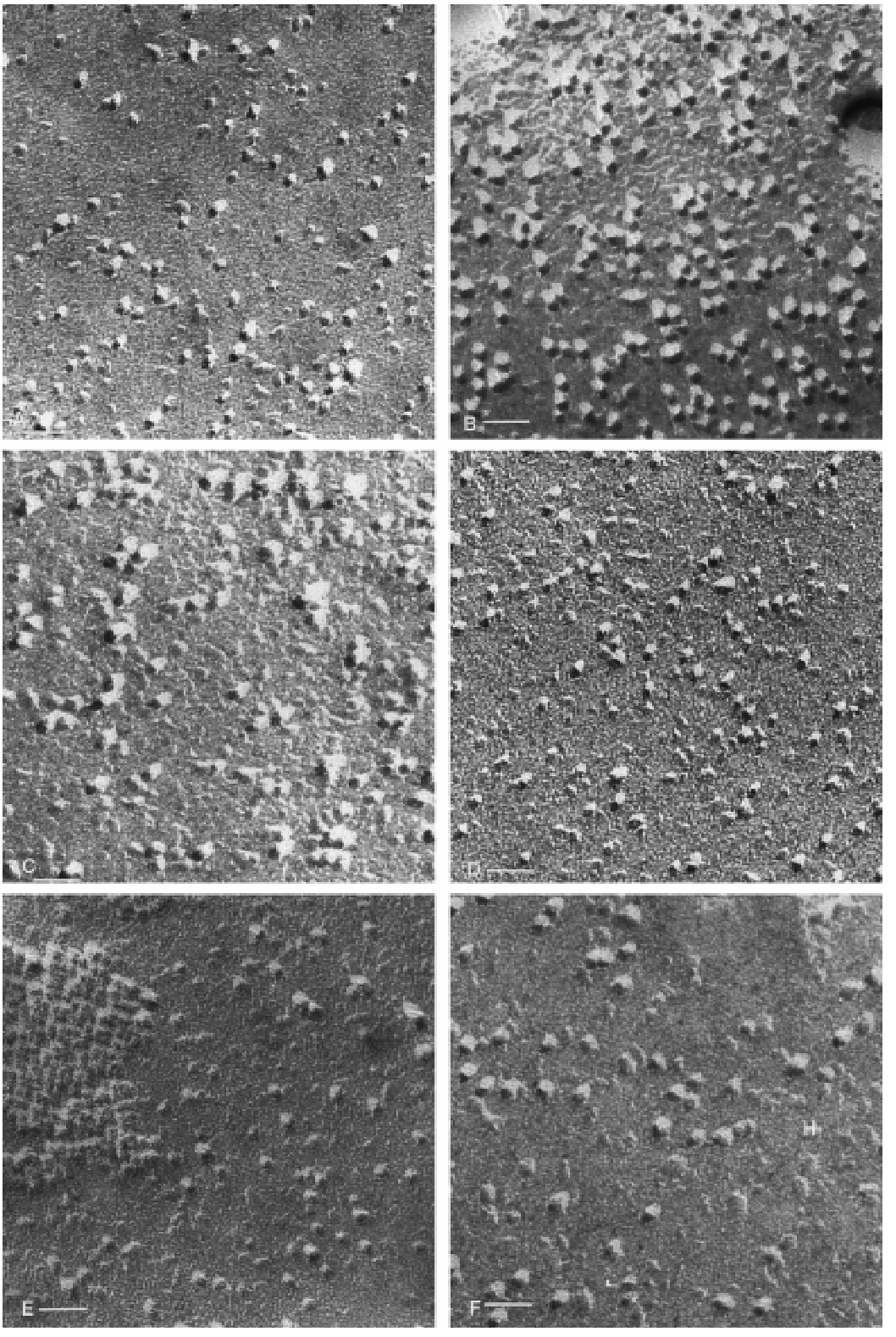

Fig. 4 Size and shape of unidirectionally shadowed freeze-fracture intramembrane particles of aquaporin-expressing cells. (*A*) mock-transfected cells with small and larger IMPs. (*B*) AQP1-expressing cells with high density of IMPs. (*C*) AQP2-expressing cells. (*D*) AQP3-expressing cells often were characterized by IMPs forming a loose cluster (right of center). (*E*) IMPs outside the OAP-aggregate of AQP4 expressing cells resemble particles inside the OAP. (*F*) AQP-5 expressing cells. *Bars*, 30 nm.

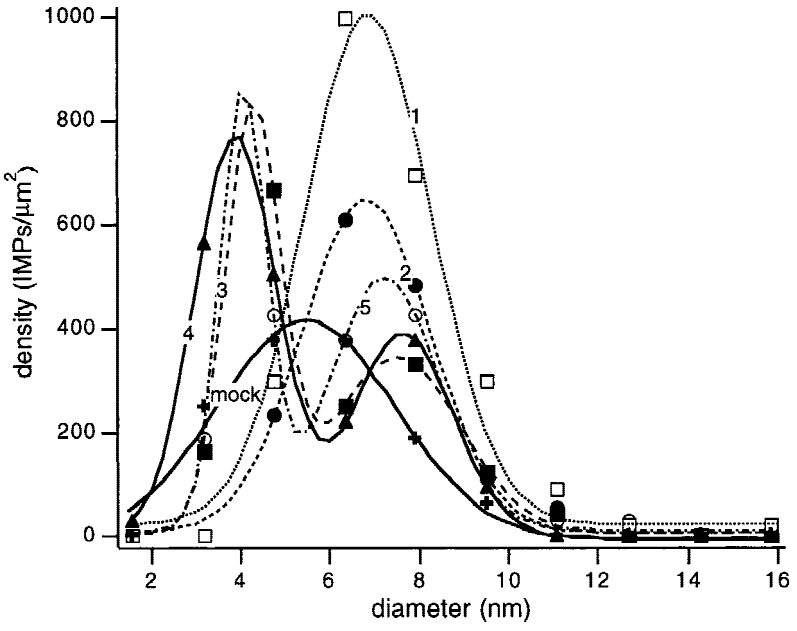

Fig. 5. Unidirectional shadowed IMP size distribution of aquaporin expressing CHO cells. IMP densities were fitted to one or two Gaussian functions. Crosses, mock transfected cells; open squares, AQP1 expressing cells; closed circles, AQP2 expressing cells; closed squares, AQP3 expressing cells; triangles, AQP4 expressing cells; open circles, AQP5 expressing cells.

Table 2. Gaussian distribution analysis of IMP-diameters from unidirectional and rotary shadowed freeze-fracture replicas

Fitted parameters	α_1	β_1	σ_1	α_2	β_2	σ_2
	(*IMPs*/μm^2)	*nm*	*nm*	(*IMPs*/μm^2)	*nm*	*nm*
Unidirectionally shadowed:						
Mock	423	5.5	2.8			
AQP1	980	6.9	2.0			
AQP2	639	6.8	2.0			
AQP3	800	4.3	0.9	339	7.5	2.0
AQP4	770	3.9	1.3	391	7.6	1.6
AQP5	836	4.1	0.7	484	7.3	1.7
Rotary shadowed:						
Mock	215	9.6	1.7	629	13.1	1.5
AQP1	1342	8.9	1.7			
AQP2	896	7.5	1.6			
AQP3	888	8.9	1.8			
AQP4	1618	7.0	0.9			
AQP5	767	8.8	2.1			

The values shown here are normalized to the values displayed in Table 1.

found, with the largest particles being present in the plasma membranes of the former. Figure 7 and Table 2 indicate that mock transfected cells had many particles of ~13 nm, but also particles of 9.5 nm. The major category of IMPs in AQP1 (Fig. 6*C*), AQP3 (Fig. 6*D*), and AQP5 (Fig. 6*F*)-transfected cells had a similar diameter of 8.9 nm, which is larger than measured in unidirectionally shadowed replicas because the thickness of the brightly shadowed rim surrounding the IMP was included. OAPs in AQP4 expressing cells (Fig. 6*E*) appeared similar to unidirectionally shadowed OAPs. The center to center spacing of the grooves in the E-face (*not shown*) and the apparent unit cell dimension in the P-face was 6.8 nm. The size distribution of IMPs in AQP2-transfected cells resembled more closely that of AQP4 than the other aquaporin transfectants (Fig. 6*C*). The abundance of relatively larger IMPs in mock transfected cells after rotary shadowing compared to smaller ones after unidirectionally shadowing cannot be ascribed to an artefactual result of rotary shadowing. The difference may be related to a specific 3 dimensional appearance of IMPs in mock transfected cells with a large base and an S or Gaussian-shaped rise from the projection plane, leading to an apparent large difference in rotary and unidirectionally shadowed projections.

Discussion

Expression of AQP1 through 5 resulted in a modification of number and size of IMPs on the plasma membrane of CHO cells as observed by freeze-fracture EM. With the exception of AQP4 transfection, which has been previously shown to result in orthogonal IMP arrays in CHO cells (Yang et al., 1996), none of the other transfected cells examined consistently showed IMP aggregates on their plasma membranes. Some small clusters were infrequently seen in AQP3-transfected cells. The AQP3 clusters had a hexagonal E-face packing, resembling gap junction connexon packing, but gap junctions have not previously been observed in the non-epithelial CHO cells in culture. Of particular interest is the observation that AQP2 did not form membrane clusters. While it is pos-

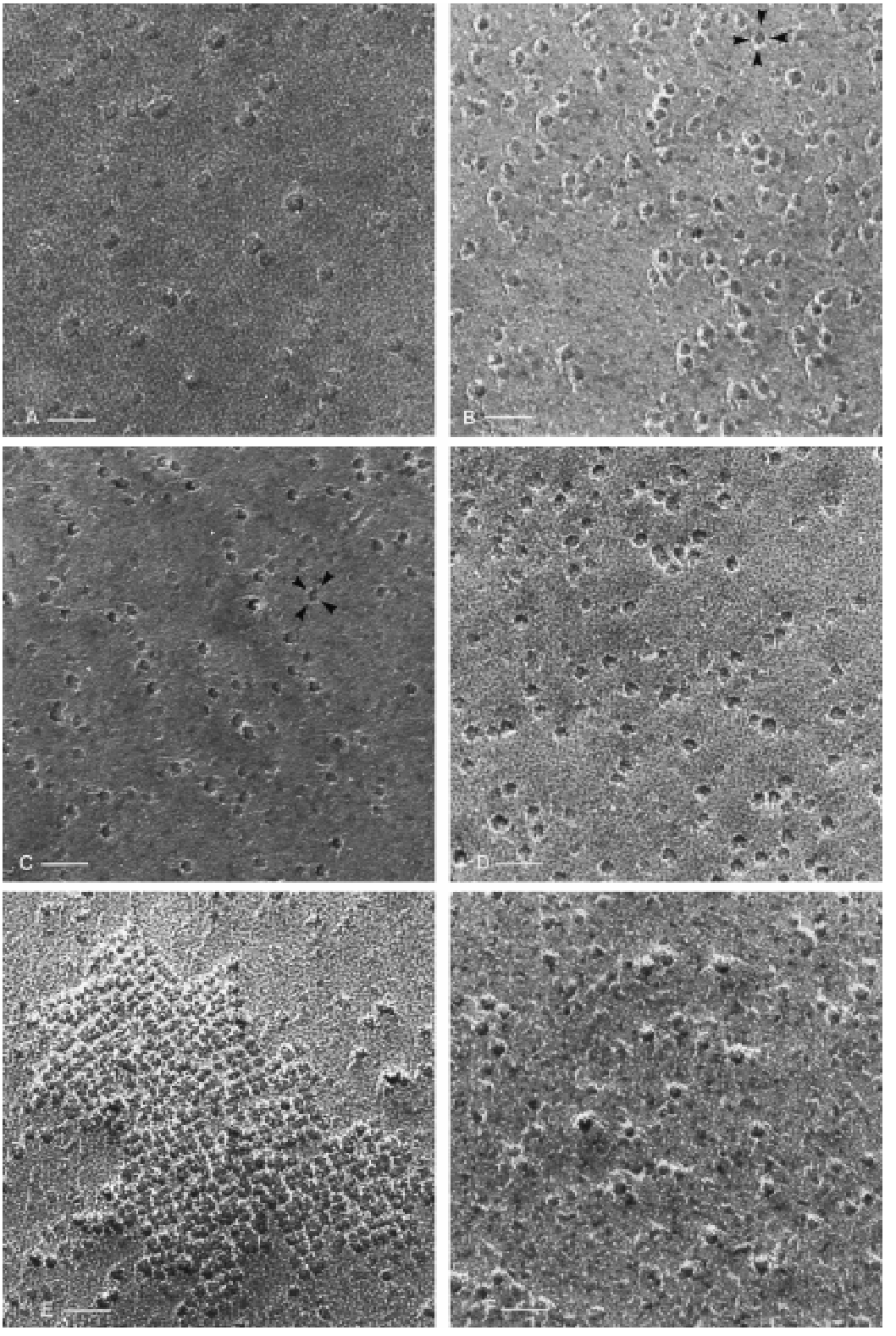

Fig. 6. Rotary shadowed freeze fracture electron micrographs of aquaporin expressing CHO cells. P-faces obtained after freeze-fracture were replicated by rotating the stage during shadowing with platinum. (*A*) mock-transfected cells showing large hexagonally shaped IMPs with a faint small shadow rim of less electron dense material; (*B*) AQP1-expressing cells, with donut-shaped IMPs. Particles having a tetrameric appearance, similarly to previously reported (Verbavatz et al., 1993) are indicated by 4 arrows; (*C*) AQP2-expressing cells with small IMPs. The shadow rims surround tetra- and pentagonal shaped particles. Features like a tetrameric assembly may be recognized (arrows); (*D*) AQP3-expressing cells, (*E*) AQP4-expressing cells, with OAPs consisting of small tetragonal-shaped structures; (*F*) AQP5-expressing cells. *Bars,* 30 nm.

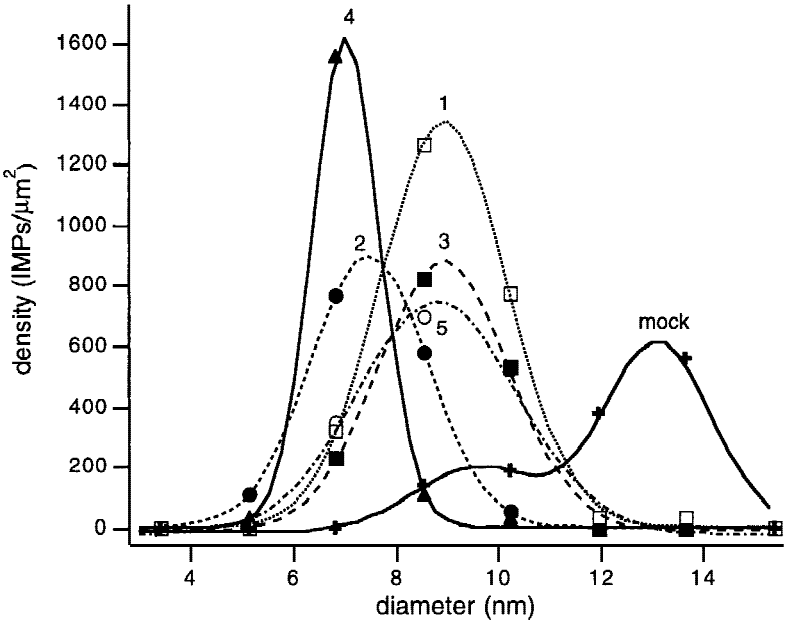

Fig. 7. Rotary shadowed IMP size distribution of aquaporin expressing CHO cells. Crosses, mock transfected cells; open squares, AQP1 expressing cells; closed circles, AQP2 expressing cells; closed squares, AQP3 expressing cells; triangles, AQP4 expressing cells; open circles, AQP5 expressing cells.

sible that the appearance of these clusters is cell-type dependent, our data show that unlike AQP4, AQP2 expression in the plasma membrane does not result in the appearance of clusters. Therefore, if the IMP clusters seen after vasopressin stimulation of principal cells indeed contain AQP2, this may reflect a speciality of these vasopressin-sensitive cells. Also, it has been proposed that the IMP clusters are located in clathrin-coated pits on the apical membrane of principal cells (Brown & Orci, 1983), and this may indicate that they appear only in cells in which the protein is being actively recycled. Thus the absence of clusters in AQP2-expressing CHO cells may reflect that fact that membrane expression of aquaporins appears to follow a constitutive, and not a regulated pathway of insertion in these cells.

A point of concern was the finding that the increases of mean particle density varied from 20 to 100%. A 20% increase, compared to a 100% increase of IMP density, may indicate poor expression of an aquaporin. Nonetheless, functional measurements suggested appreciable amounts of aquaporins appearing on plasma membranes, given the knowledge of single channel water permeabilities (Yang & Verkman, 1997) in combination with the more than 5-fold increases of perfusion-limited aquaporin-mediated osmotic water permeabilities reported in Fig. 1. Size frequency analyses revealed significant differences with respect to mock-transfected cells, suggesting that changes in density are not as important as size and shape in determining the effect of protein transfection on plasma membrane composition. Thus, transfection may lead to a decreased delivery of other proteins to the membrane, so that upon aquaporin expression the actual number of IMPs does not change markedly. Their size/function does, however, reflect the increased number of IMPs that are due to aquaporin expression. In the *Xenopus* oocyte expression system, though, water-injected oocytes exhibited an extremely low density of endogenous IMPs with a 2 to 20 times increase of IMPs upon exogenous expression of channels and transporters (Zampighi et al., 1995).

We have previously shown that AQP1 forms tetramers in lipid bilayers. A similar arrangement was found in proteoliposomes after AQP1 was enzymatically deglycosylated (van Hoek et al., 1995). Two-dimensional crystallography confirmed that detergent solubilized deglycosylated AQP1 monomers pack as tetramers in the bilayer plane in a tetragonal crystalline lattice (Cheng et al., 1997). Such an arrangement could not be established for all aquaporin expressing membranes in this study. It was not possible to identify IMPs as defined proteins because the membranes of CHO cells contain proteins other than the aquaporins. This identification process is made more difficult by the fact that the appearance of a tetrameric arrangement also depends on several technical parameters such as the angle of specimen tilt in the microscope. Thus, even in liposomes that contain only a single protein, AQP1, all of the IMPs in a single image do not appear as tetramers. Upon modifying the tilt angle, the tetrameric assembly becomes apparent in many cases (Verbavatz et al., 1993). Such an analysis would be virtually impossible to achieve in a membrane containing a heterogeneous population of IMPs, such as the transfected CHO cells.

Aquaporin expression in CHO cells resulted in general changes of IMP appearances with a shift towards a larger apparent particle size in the plasma membrane

after unidirectional shadowing and a smaller particle size after rotary shadowing. In addition, different-sized particles were also found in some aquaporin expressing cells and may indicate that the cohort of IMPs expressed on the plasma membranes of transfected cells is modified beyond the simple addition of a new protein. The measurements of IMP diameters reported here and in previous studies depend on the techniques used to prepare the replicas. The diameter of any IMP measured by unidirectional shadowing does not depend upon the height of the IMP (i.e., its projection out of the plane of the replica). This is because the diameter is measured at right angles to the direction of shadowing. However, in rotary shadowed specimens, the taller the IMP, the greater will be its apparent diameter because it casts a longer shadow around its total circumference. This may explain the difference in IMP diameters measured in aquaporin expressing cells using the two techniques. An unprecedented finding was that a population of apparently very large IMPs after rotary shadowing in the mock transfected cells looked very different from those after unidirectional shadowing beyond the intrinsic difference generated by the various techniques to prepare replicas. This suggests distinctive 3-dimensional shapes of these particles that are revealed differently by unidirectional and rotary shadowing and indicate that both techniques may complement each other in assessing the 3-dimensional shape of an IMP. Whatever the exact shape of the majority of IMPs of mock-transfected cells, they appear quite different in conventional and rotary shadowed replicas, contrary to IMPs of aquaporin-expressing cells, which appear more similar in size using the two different shadowing techniques. This finding provides additional support for the proposed transfection-induced alteration in IMP profile of the plasma membrane.

In conclusion, aquaporin (1–5) expression led to morphological modifications of the cell plasma membrane with respect to number and size of intramembrane particles. Only AQP4 aggregates into orthogonal arrays. Size determination of IMPs suggests that the other aquaporins may form tetramers in the plasma membrane, but the question whether all aquaporins form tetramers in the plasma membrane must await purification and reconstitution into liposomes, as has been achieved for AQP1 and AQP4 (Yang, van Hoek & Verkman, 1997). Comparative studies utilizing CHO cell-expressing aquaporins will be useful to support further structure/function studies in various tissues, and AQP-knockout mice that are currently available or are being developed.

This work was supported by National Institutes of Health Research Grant R01 DK 55864 and Program Grant, Project 1, DK38452. B.Y. and S.K. were supported by NIH-DK35124 to Dr. A.S. Verkman. We thank Dr. A.S. Verkman for critical reading of the manuscript.

References

Agre, P., Brown, D., Nielsen, S. 1995. Aquaporin water channels: unanswered questions and unresolved controversies. *Curr. Opin. Cell. Biol.* **7:**472–483

Bartels, H. 1979. The air-blood barrier in the human lung. A freeze-fracture study. *Cell Tissue Res.* **198:**269–285

Bordi, C., Perrelet, A. 1978. Orthogonal arrays of particles in plasma membranes of the gastric parietal cell. *Anat. Rec.* **192:**297–303

Brown, D., Grosso, A., DeSousa, R.C. 1983. Correlation between water flow and intramembrane particle aggregates in toad epidermis. *Am. J. Physiol.* **245:**C334–C342

Brown, D., Orci, L. 1983. Vasopressin stimulates formation of coated pits in rat kidney collecting ducts. *Nature* **302:**253–255

Brown, D. 1991. Structural-functional features of antidiuretic hormone-induced water transport in the collecting duct. *Semin. Nephrol.* **11:**478–501

Cheng, A., Van Hoek, A.N., Yeager, M., Verkman, A.S., Mitra, A.K. 1997. Three-dimensional organization of a human water channel. *Nature* **387:**627–630

Chevalier, J., Bourguet, J., Hugon, J.S. 1974. Membrane associated particles: distribution in frog urinary bladder epithelium at rest and after oxytocin treatment. *Cell Tissue Res.* **152:**129–140

Ehring, G.R., Zampighi, G., Horwitz, J., Bok, D., Hall, J.E. 1990. Properties of channels reconstituted from the major intrinsic protein lens fiber membranes. *J. Gen. Physiol.* **96:**631–664

Ellisman, M.H., Rash, J.E., Staehelin, L.A., Porter, K.R. 1976. Studies of excitable membranes. II. A comparison of specializations at neuromuscular junctions and nonjunctional sarcolemmas of mammalian fast and slow twitch muscle fibers. *J. Cell Biol.* **68:**752–774

Farinas, J., Kneen, M., Moore, M., Verkman, A.S. 1997. Plasma membrane water permeability of cultured cells and epithelia measured by light microscopy with spatial filtering. *J. Gen. Physiol.* **110:**283–296

Forge, A. 1987. Specializations of the lateral membrane of inner hair cells. *Hear. Res.* **31:**99–109

Frigeri, A., Gropper, M., Umenishi, F., Kawashima, M., Brown, D., Verkman, A.S. 1995. *J. Cell Sci.* **108:**2993–3002

Harmanci, M.C., Stern, P., Kachadorian, W.A., Valtin, H., DiScala, V.A. 1978. Antidiuretic hormone-induced intramembranous alteration in mammalian collecting ducts. *Am. J. Physiol.* **235:**F440–F443

Harmanci, M.C., Stern, P., Kachadorian, W.A., Valtin, H., DiScala, V.A. 1980. Vasopressin and collecting duct intramembranous particle clusters: a dose-response relationship. *Am. J. Physiol.* **239:**F560–F564

Hirsch, M., Gache, E., Noske, W. 1988. Orthogonal arrays of particles in non-pigmented cells of rat ciliary epithelium: relation to distribution of filipin- and digitonin-induced alterations of the basolateral membrane. *Cell Tissue Res.* **252:**165–173

Humbert, F., Pricam, C., Perrelet, A., Orci, L. 1975. Specific plasma membrane differentiations in the cells of kidney collecting tubule. *J. Ultrastr. Res.* **52:**13–20

Kachadorian, W.A., Wade, J.B., DiScala, V.A. 1975. Vasopressin: induced structural change in toad bladder luminal membrane. *Science* **190:**67–69

Knepper, M.A., Wade, J.B., Terris, J., Ecelbarger, C.A., Marples, D., Mandon, B., Chou, C.L., Kishore, B.K., Nielsen, S. 1996. Renal aquaporins. *Kidney Int.* **49:**1712–1717

Landis D.M., Reese, T.S. 1981. Membrane structure in mammalian astrocytes: a review of freeze-fracture studies on adult, developing, reactive and cultured astrocytes. *J. Exp. Biol.* **95:**35–48

Ma, T., Frigeri, A., Tsai, S.T., Verbavatz, J.M., Verkman, A.S. 1993.

Localization and functional analysis of CHIP28k water channels in stably transfected Chinese hamster ovary cells. *J. Biol. Chem.* **268:**22756–22764

Orci, L., Humbert, F., Brown, D., Perrelet, A. 1981. Membrane ultrastructure in urinary tubules. *Int. Rev. Cytol.* **73:**183–242

Saito, K. 1988. Orthogonal arrays of intramembrane particles in the supporting cells of the guinea-pig vestibular sensory epithelium. *Am. J. Anat.* **183:**338–343

Schmalbruch J. 1979. 'Square arrays' in the sarcolemma of human skeletal muscle fibres. *Nature* **281:**145–146

Staehelin, L.A. 1972. Three types of gap junctions interconnecting intestinal epithelial cells visualized by freeze-etching. *Proc. Natl. Acad. Sci. USA* **69:**1318–1321

Van Hoek, A.N., Wiener, M.C., Verbavatz, J.M., Brown, D., Lipniunas, P.H., Townsend, R.R., Verkman, A.S. 1995. Purification and structure-function analysis of native, PNGase F- and endo-β-galactosidase-treated CHIP28 water channels. *Biochemistry* **34:**2212–2219

Van Os, C.H., Deen, P.M.T., Dempster, J.A. 1994. Aquaporins: water selective channels in biological membranes. Molecular structure and tissue distribution. *Biochim. Biophys. Acta* **1197:**291–309

Verbavatz, J.M., Brown, D., Sabolic, I., Valenti, G., Van Hoek, A.N., Ma, T., Verkman, A.S. 1993. Tetrameric assembly of CHIP28 water channels in liposomes and cell membranes. A freeze-fracture study. *J. Cell Biol.* **123:**605–618

Verbavatz, J.M., Ma, T., Gobin, R., Verkman, A.S. 1997. Absence of orthogonal arrays in kidney, brain and muscle from transgenic knockout mice lacking water channel aquaporin-4. *J. Cell Sci.* **110:**2855–2860

Verkman, A.S., Van Hoek, A.N., Ma, T., Frigeri, A., Skach, W.R., Mitra, A., Tamarappoo, B.K., Farinas, J. 1996. Mechanisms of water transport across mammalian cell membranes. *Am. J. Physiol.* **270:**C12–C30

Widdicombe, J.H., Coleman, D.L., Finkbeiner, W.E., Friend, D.S. 1987. Primary cultures of the dog's tracheal epithelium: fine structure, fluid, and elctrolyte transport. *Cell Tissue Res.* **247:**95–103

Yang, B., Brown, D., Verkman, A.S. 1996. The mercurial insensitive water channel (AQP-4) forms orthogonal arrays in stably transfected chinese hamster ovary cells. *J. Biol. Chem.* **271:**4577–4580

Yang, B., Verkman, A.S. 1997. Water and glycerol permeabilities of aquaporins 1-5 and MIP determined quantitatively by expression of epitope-tagged constructs in *Xenopus* oocytes. *J. Biol. Chem.* **272:**16140–16146

Yang, B., Van Hoek, A.N., Verkman, A.S. 1997. Very high single channel water permeability of aquaporin-4 in baculovirus-infected insect cells and liposomes reconstituted with purified aquaporin-4. *Biochemistry* **36:**7625–7632

Zampighi G., Simon, S.A., Robertson, J.D., McIntosh, T.J., Costello, M.J. 1982. On the structural organization of isolated bovine lens fiber junctions. *J. Cell Biol.* **93:**175–189

Zampighi, G.A., Kreman, M., Boorer, K.J., Loo, D.D.F., Bezanilla, F., Hall, J.E., Wright, E.M. 1995. A method for determining the Unitary Functional Capacity of cloned channels and transporters expressed in *Xenopus laevis* oocytes. *J. Membrane Biol.* **148:**65–78